AD_____

Award Number: W81XWH-05-1-0592

TITLE: PSMA-Targeted Nano-Conjugates as Dual-Modality (MRI/PET) Imaging Probes for the Non-Invasive Detection of Prostate Cancer

PRINCIPAL INVESTIGATOR: Xiankai Sun, Ph.D.

CONTRACTING ORGANIZATION: University of Texas Southwestern Medical Center at Dallas
Dallas, Texas 75390-9058

REPORT DATE: October 2007

TYPE OF REPORT: Annual

PREPARED FOR: U.S. Army Medical Research and Materiel Command
Fort Detrick, Maryland 21702-5012

REPORT DOCUMENTATION PAGE

Form Approved
OMB No. 0704-0188

1. REPORT DATE *(DD-MM-YYYY)*	**2. REPORT TYPE**	**3. DATES COVERED** *(From - To)*
01-10-2007	Annual	15 OCT 2006 - 14 SEP 2007

4. TITLE AND SUBTITLE

PSMA-Targeted Nano-Conjugates as Dual-Modality (MRI/PET) Imaging Probes for the Non-Invasive Detection of Prostate Cancer

5a. CONTRACT NUMBER

5b. GRANT NUMBER
W81XWH-05-1-0592

5c. PROGRAM ELEMENT NUMBER

6. AUTHOR(S)
Xiankai Sun, Ph.D.

E-Mail: Xiankai.Sun@UTSouthwestern.edu

5d. PROJECT NUMBER

5e. TASK NUMBER

5f. WORK UNIT NUMBER

7. PERFORMING ORGANIZATION NAME(S) AND ADDRESS(ES)

University of Texas Southwestern Medical Center at Dallas
Dallas, Texas 75390-9058

8. PERFORMING ORGANIZATION REPORT NUMBER

9. SPONSORING / MONITORING AGENCY NAME(S) AND ADDRESS(ES)
U.S. Army Medical Research and Materiel Command
Fort Detrick, Maryland 21702-5012

10. SPONSOR/MONITOR'S ACRONYM(S)

11. SPONSOR/MONITOR'S REPORT NUMBER(S)

12. DISTRIBUTION / AVAILABILITY STATEMENT
Approved for Public Release; Distribution Unlimited

13. SUPPLEMENTARY NOTES

14. ABSTRACT
The goal of this project is to develop dual modality imaging probes for the detection of prostate cancer by doping radioisotopes to iron oxide nanoparticles, so that the sensitivity and specificity of prostate cancer diagnosis could be significantly improved. In the second year, a rigorous synthetic protocol has been developed to prepare dextran T10-coated iron oxide nanoparticles with uniform size distribution and better controllable reproducibility compared to the method developed in the first year. Protocol of conjugating nanoparticles with prostate cancer targeting molecules has been successfully established. Two nanoparticles with mean sizes of 11.8 and 30.6 nm (radii) were evaluated in vitro and in vivo. The relaxivity values (r2) of the prepared nanoparticles were observed up to 43.3 mM-1s-1 with the r2/r1 ratio being 88.4, exhibiting potential application of contrast enhancement on T2- and T2*-weighted MR images. Both nanoparticles showed excellent in vitro stability in rat serum. The biodistribution studies in normal animal showed that the smaller nanoparticle (NP-1, radius 11.8 nm) has a better tissue distribution profile than the larger one (NP-2, radius 30.6 nm). Impressively, NP-1 showed remarkable tumor uptake in a PC-3 xenograft model with a tumor to muscle ratio of 12.11 ± 3.87 at 24 h post injection.

15. SUBJECT TERMS
No subject terms provided.

16. SECURITY CLASSIFICATION OF:			**17. LIMITATION OF ABSTRACT**	**18. NUMBER OF PAGES**	**19a. NAME OF RESPONSIBLE PERSON**
a. REPORT	**b. ABSTRACT**	**c. THIS PAGE**			USAMRMC
U	U	U	UU	12	**19b. TELEPHONE NUMBER** *(include area code)*

Standard Form 298 (Rev. 8-98)
Prescribed by ANSI Std. Z39.18

Table of Contents

Introduction

The goal of this project was set to explore a new approach that will combine the advantages of MRI and PET for the diagnostic imaging and staging of prostate cancer. We propose to dope positron-emitting isotopes to superparamagnetic iron oxide nanoparticle to make nanosized dual MRI/PET probes for the detection of prostate cancer by multi-modality (anatomical MRI plus functional PET) molecular imaging approaches, so that the sensitivity and specificity of prostate cancer diagnosis could be significantly improved. To realize the goal, two objectives were specified for this project: **Objective I**. Preparation/characterization of $^{77/74}$As-doped iron oxide nanoparticles and construction of PSMA-targeted nano-conjugates; and **Objective II**. Evaluation of the PSMA-targeted nano-conjugates in prostate cancer xenograft mouse models via conventional biodistribution and small animal MRI/PET imaging methods.

Body

In the statement of work (SOW), the focus of our second year work was on part of **Objective I** and **Objective II.** Specifically,

Months 6 – 15:

Milestone 2: Establish protocols of making dextran-coated $^{77/74}$As-doped iron oxide nanoparticles to obtain optimal conditions to control the incorporation ratio of $^{77/74}$As into the iron oxide core.

Months 9 – 18:

Milestone: Establish protocols to construct PSMA-targeted nano-conjugates. Four such nano-conjugates are anticipated (two nano-conjugates with sizes of 25 nm and 35 nm per targeting molecule).

Months 12 – 30:

Milestone: Accomplish the in vitro/in vivo evaluations of the four PSMA-targeted nano-conjugates. At the end of this timeframe, we will be able to tell which targeting approach is better. We anticipate two nano-conjugates (one per targeting molecule) that can be used for small animal imaging studies.

Research Progress in the Second Year:

Months 6 – 15:

Milestone 2 (completed in the 1st year but further optimized in the 2nd year): Establish protocols of making dextran-coated $^{77/74}$As-doped iron oxide nanoparticles to obtain optimal conditions to control the incorporation ratio of $^{77/74}$As into the iron oxide core.

The determinants of nanoparticle size have been identified

In the first year, we primarily used a dextran with molecular weight (MW) range of 64 – 76 KDa for the synthesis of iron oxide based nanoparticle. As reported in the first year, factors such as concentration, pH, temperature, and reaction time had been evaluated. The results showed that only concentration affects the final particle size. Due to the broad dextran MW range, the prepared nanoparticle size distribution could be broaden accordingly. Therefore, in the second year, we tested another dextran, T10 (MW: 10 KDa), which has been approved by the FDA for

the formulation of iron oxide based T2 MRI contrast agents. Interestingly, when using T10 for iron oxide nanoparticle coating, the nanoparticle size is only determined by the amount of T10 used if the Fe^{3+}/Fe^{2+}concentration is fixed. This makes the size and size distribution control much easier. Compared with the method of using the 64-76 KDa dextran, the T10 procedures can provide nanoparticles with more uniform size distribution (Figure 1), and can be well controlled and reproduced. Therefore the T10 dextran was chosen for the further study.

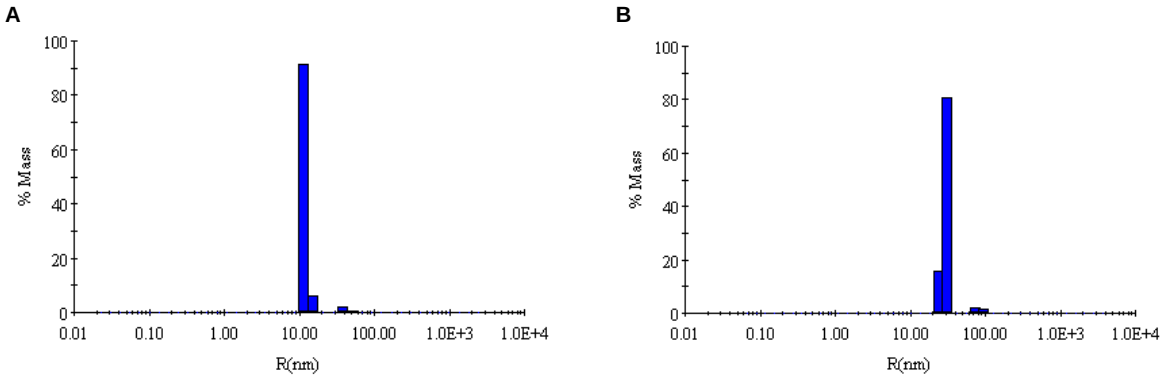

Figure 1. DLS results of two different sizes of ^{177}Lu-doped T10-coated iron oxide nanoparticles (A) small size (NP-1: 11.8 ±1.3 nm, 97.2%) and (B) large size (NP-2: 30.6 ± 0.5 nm; 96.3%).

Nuclear imaging isotopes have been successfully doped into the T10-coated nanoparticles

The incorporation yields of ^{77}As, ^{177}Lu, ^{64}Cu and ^{111}In were comparable to the nanoparticles coated with the 64-76 KDa dextran. Specifically, the incorporation ratios for a typical PET isotope ^{64}Cu and ^{177}Lu were about 50% and 73 %, respectively, with a total preparation time of 4 hours. After purification, HPLC, TEM, AFM, and DLS characterization results demonstrated that the particle size distribution was narrow and the radioisotope was incorporated into nanoparticles without non-specifically bound metal ions. The ^{177}Lu-doped T10-coated nanoparticles (NP-1 and NP-2) were used for the following *in vitro* and *in vivo* evaluation.

Months 9 – 18:

Milestone: Establish protocols to construct PSMA-targeted nano-conjugates. Four such nano-conjugates are anticipated (two nano-conjugates with sizes of 25 nm and 35 nm per targeting molecule).

Conjugation protocol has been established by using a prostate cancer targeting peptide, NH_2G-R11.

By in vivo evaluation of NP-1 and NP-2, we found that NP-1 showed an optimal tissue distribution profile in comparison to NP-2. Therefore we used NP-1 as platform to construct a prostate cancer targeted nanoconjugate by using a peptide, NH_2G-R11.

Protocol established: The purified and concentrated T10-coated iron oxide nanoparticle was reacted with 1 M chloroacetic acid in 3 M NaOH for 16 h at room temperature in order to introduce carboxylate groups in the dextran chains. Unreacted chloroacetic acid was removed by repeated YM-100 centricon washing via Milli-Q water (3 × 2 mL), and then a DMSO water

solution (DMSO/Water, v/v = 1:1). The carboxylate groups on the surface of nanoparticle were activated with NHS/EDC for 15 min. To the activated ester solution, 3 μL of NH_2G-R11 (10 μg/ μL in DMSO) was added. The resulting mixture was shaken at 650 rpm at RT for 3 h. The following purification was done by YM-100 centricon wash. The reaction was monitored by size exclusion HPLC using UV, Light Scattering, and radioactivity detectors (Figure 2).

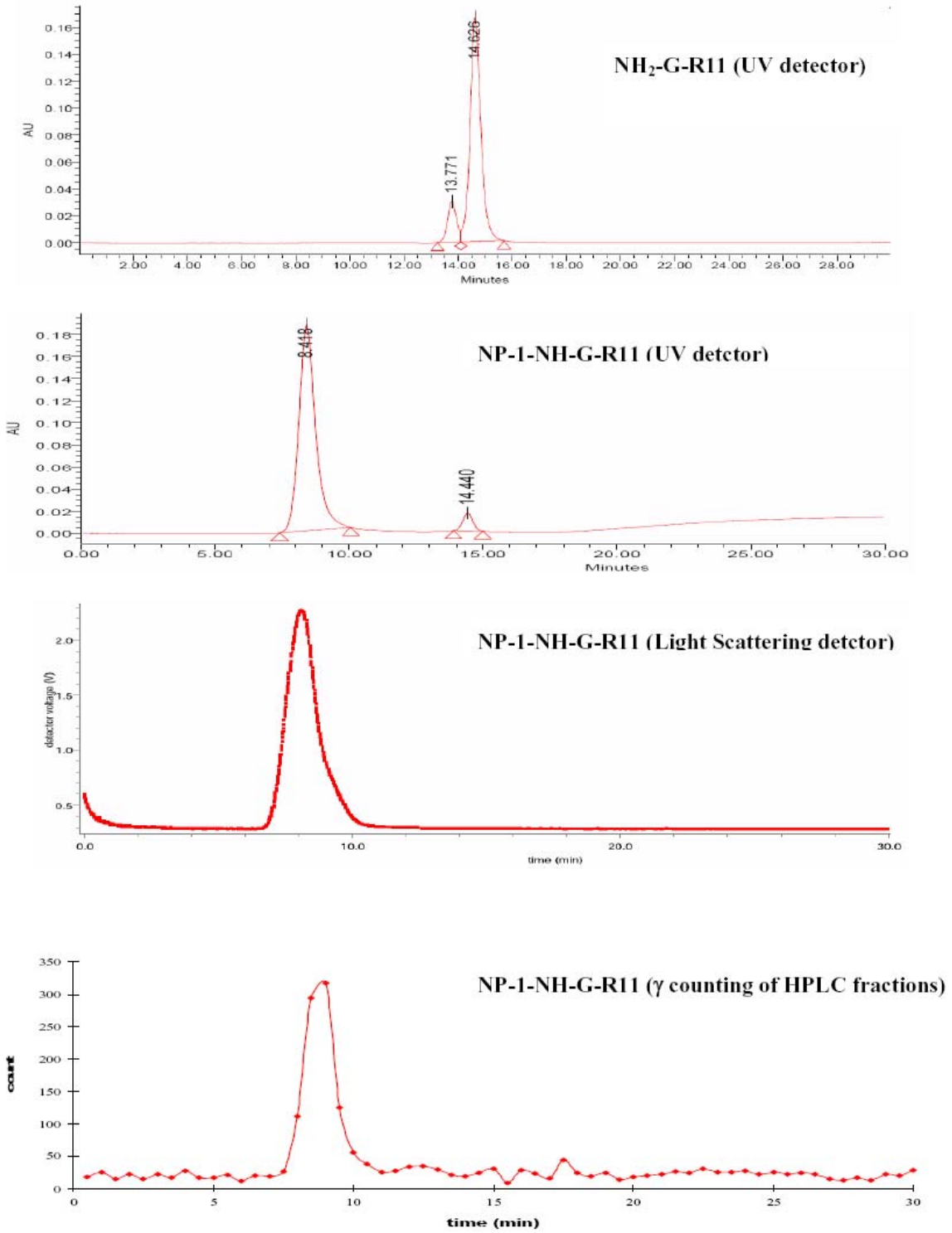

Figure 2. Size exclusion HPLC monitoring of the conjugation of NP-1 with a prostate cancer targeting peptide, NH_2G-R11.

Figure 2 evidently demonstrates that the prostate cancer targeting peptide, NH2G-R11, has been successfully conjugated to the ^{177}Lu-doped NP-1 nanoparticle. Two prostate cancer targeting molecules, E6 (a PSMA antibody) and xPSM-A10-3 (a PSMA-specific aptamer), were proposed in this project. Dr. Philip Thorpe laboratory provided us 10-mg of E6 antibody for our work. However, the antibody didn't show positive staining on C4-2 cells due to somewhat reasons that probably occurred in the antibody production. We reported this to Dr. Thorpe. His laboratory will start a new production soon. Once we get the antibody, we will use the conjugation protocol to prepare E6 nanoconjugates. The conjugation with xPSM-A10-3 will be also carried out in the same way in the third year.

Months 12 – 30:

Milestone: Accomplish the in vitro/in vivo evaluations of the four PSMA-targeted nano-conjugates. At the end of this timeframe, we will be able to tell which targeting approach is better. We anticipate two nano-conjugates (one per targeting molecule) that can be used for small animal imaging studies.

In vitro stability of NP-1 and NP-2 has been evaluated.

The in vitro stability of both NP-1 and NP-2 have been evaluated in rat serum and PBS. Both particles exhibited excellent in vitro stability by staying > 92% intact in rat serum and >99% in PBS out to 72 h. The experiments were carried out in triplicate.

Magnetic Resonance (MR) relaxivities (r1 and r2) of NP-1 and NP-2 has been measured.

The magnetic resonance relaxivity of the nanoparticles was measured by a 4.7 T magnet. A series of NP dilutions were prepared and transferred into a 9-well plate. T1 and T2 weighted imaging was performed (Figure 3).

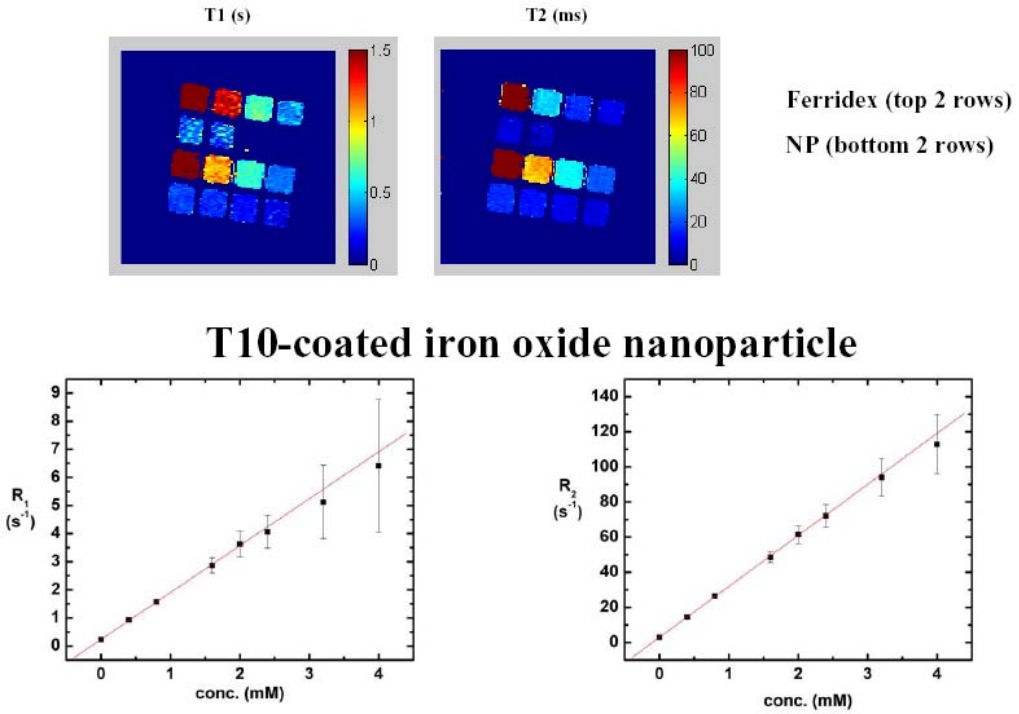

Figure 3. Relaxivity values determination of T10-coated nanoparticle (NP-1). The commercial iron oxide particle (Ferridex) was used as reference.

The relaxivity of nanoparticles coated with the 64-76 KDa dextran and T10 dextran were measured. The results are summarized in Table 1. It looks that the 64-76 KDa dextran coated nanoparticles have higher r2 value than the T10 coated one. This is likely due to the bigger size of the 64-76 KDa dextran coated nanoparticles (DLS: 15 nm vs NP-1's DLS: 11.8 nm). Likely there are likely more iron atoms in the 64-76 KDa dextran coated nanoparticles. Both nanparticles showed high r2/r1 ratios demonstrating the potential of such nanoparticles for T2 contrast enhancement of MR imageing.

Table 1. Magnetic Resonance (MR) relaxivities (r1 and r2) measured at 4.7 T (200 MHz).

NP size (radius) & Dextran used (MW)	**Longitudinal relaxivity (r1) $mM^{-1}s^{-1}$**	**Transverse relaxivity (r2) $mM^{-1}s^{-1}$**	**r2/r1**
~15 nm 64~76 KDa	0.49 ± 0.04	43.3 ± 1.8	88.4
~ 10 nm T10 (10 KDa)	0.64 ± 0.04	13.6 ± 0.4	21.3

In vivo tissue distribution of NP-1 and NP-2 has been evaluated in mice.

All animal studies were performed in compliance with guidelines set by the UT Southwestern Animal Studies Committee. Two different sizes of ^{177}Lu-doped nanoparticles (small size: NP-1 and large size: NP-2) were used for the in vivo evaluation. Both NP-1 and NP-2 were diluted with 10 mM PBS to prepare injection does. Normal 4–5 wk male healthy BALB/c mice (Harlan, IN) were injected with 100 μL of NP-1 or NP-2 (~ 5 μCi) via the tail vein. The animals were anesthetized prior to sacrifice at each time point. Organs of interest (blood, lungs, liver, spleen, kidneys, fat, muscle, heart, intestines and stomach) were removed, weighed, and counted. Standards were prepared and counted along with the samples to calculate the percent injected dose per gram tissue (%ID/g) and percent injected dose per organ (%ID/organ). Four time points (1 h, 4 h, 24 h, and 48 h; n = 4) were used for the evaluation. The animals of the last time point groups were housed in metabolic cages to collect urine and feces at 1 h, 4 h, 24 h and 48 h p.i.

The biodistribution results of NP-1 and NP-2 are presented in Table 5, Table 6, and Figure 7). At early time points (1 h and 4 h), NP-1 showed significant higher accumulation in blood (NP-1: 39.29 ± 0.84 %ID/g at 1 h p.i. and 23.29 ± 1.99 %ID/g at 4 h p.i.; NP-2: 5.34 ± 0.38 %ID/g at 1 h p.i and 1.11 ± 0.12 %ID/g at 4 h p.i.) and less deposition in liver (NP-1: 9.24 ± 1.12 %ID/g at 1 h p.i. and 18.41 ± 0.58 %ID/g at 4 h p.i.; NP-2: 43.45 ± 3.55 %ID/g at 1 h p.i. and 32.80 ± 3.88 %ID/g at 4 h p.i.), and less uptake in spleen (NP-1: 5.83 ± 0.36 %ID/g at 1 h p.i. and 12.61 ± 2.19 %ID/g at 4 h p.i.; NP-2: 30.05 ± 1.36 %ID/g at 1 h p.i. and 20.20 ± 4.85 %ID/g at 4 h p.i.) than NP-2. No significant fat, muscle, heart, intestines and stomach uptake was observed for either NP-1 or NP-2. A prolonged retention time of nanoparticle in the bloodstream is desired for the nanoconjugate to reach their targets and then enables tumor diagnosis. Due to the presence of organs of the reticuloendothelial system (RES), the particles should have retarded opsonization and macrophage recognition to avoid rapid clearance from the bloodstream. Compared to NP-2, NP-1 has shown an optimal tissue distribution profile for further evaluation.

Table 1. The biodistribution of NP-1 in normal BALB/c mice (n = 4). Data are presented as %ID/g ± s.d. and %ID/organ ± s.d.

organ	%ID/g				%ID/organ			
	1 h	4 h	24 h	48 h	1 h	4 h	24 h	48 h
blood	39.29 ± 0.84	23.29± 1.99	1.06 ± 0.02	0.12 ± 0.03	57.53 ± 0.29	37.18 ± 3.01	1.52 ± 0.03	0.18 ± 0.05
lung	11.93 ± 0.82	7.44 ± 0.62	1.73 ± 0.31	1.59 ± 0.55	1.56 ± 0.20	1.09 ± 0.16	0.23 ± 0.07	0.25 ± 0.09
liver	9.24 ± 1.12	18.41± 0.58	22.54 ± 1.93	19.07 ± 0.18	8.04 ± 0.84	20.04 ± 1.16	22.21 ± 2.74	22.38 ± 3.35
spleen	5.83 ± 0.36	12.61± 2.19	23.01 ± 2.87	26.85± 0.77	0.38 ± 0.01	1.03 ± 0.04	1.63 ± 0.31	1.71 ± 0.14
kidney	7.30 ± 0.93	4.99 ± 0.19	2.71 ± 0.29	3.00 ± 2.05	2.01 ± 0.21	1.75 ± 0.16	0.80 ± 0.16	0.98 ± 0.54
muscle	0.49 ± 0.08	0.63 ± 0.23	0.27 ± 0.07	0.37 ± 0.17	4.36 ± 0.76	5.97 ± 2.37	2.26 ± 0.55	3.18 ± 1.37
fat	0.46 ± 0.10	0.43 ± 0.11	0.27 ± 0.06	0.18 ± 0.03	1.42 ± 0.27	1.36 ± 0.27	0.76 ± 0.18	0.54 ± 0.07
heart	4.62 ± 0.53	4.41 ± 0.76	1.28 ± 0.28	0.98 ± 0.31	0.49 ± 0.06	0.54 ± 0.13	0.12 ± 0.03	0.11 ± 0.03
stomach	1.60 ± 0.34	1.25 ± 0.35	0.95 ± 0.14	0.78 ± 0.20	0.34 ± 0.04	0.34 ± 0.00	0.27 ± 0.03	0.17 ± 0.03
intestines	1.25 ± 0.08	0.97 ± 0.31	0.68 ± 0.06	0.87 ± 0.55	2.09 ± 0.02	1.99 ± 0.48	1.39 ± 0.20	1.50 ± 0.55

Table 6. The biodistribution of NP-2 in normal BALB/c mice (n = 4). Data are presented as %ID/g ± s.d. and %ID/organ ± s.d.

organ	%ID/g				%ID/organ			
	1 h	4 h	24 h	48 h	1 h	4 h	24 h	48 h
blood	5.34 ± 0.38	1.11 ± 0.12	0.09 ± 0.01	0.05 ± 0.01	6.65 ± 0.47	1.60 ± 0.25	0.13 ± 0.01	0.08 ± 0.02
lung	7.40 ± 0.82	3.12 ± 0.43	1.22 ± 0.21	1.36 ± 0.20	0.94 ± 0.11	0.39 ± 0.05	0.17 ± 0.02	0.18 ± 0.04
liver	43.45 ±3.55	32.80 ± 3.88	40.57 ± 6.02	36.80 ± 1.88	41.74 ±1.70	36.27 ± 3.95	40.18 ± 2.33	40.68 ± 1.20
spleen	30.05±1.36	20.20 ± 4.85	25.78 ± 3.88	24.69 ± 4.04	2.05 ± 0.23	1.55 ± 0.72	1.90 ± 0.50	1.40 ± 0.64
kidney	3.47 ±0.34	3.20 ± 0.62	1.91 ± 0.17	1.23 ± 0.19	0.94 ± 0.03	0.95 ± 0.22	0.52 ± 0.10	0.36 ± 0.05
muscle	1.60 ±0.42	0.56 ± 0.08	0.61 ± 0.18	0.56 ± 0.11	11.72 ±3.18	4.70 ± 0.80	5.26 ± 1.72	4.93 ± 1.04
fat	0.58 ± 0.10	0.29 ± 0.19	0.33 ± 0.18	0.50 ± 0.46	1.43 ± 0.27	0.82 ± 0.52	0.96 ± 0.55	1.45 ± 1.31
heart	1.13 ± 0.60	0.53 ± 0.09	0.43 ± 0.09	0.71 ± 0.66	0.13 ± 0.03	0.09 ± 0.04	0.04 ± 0.01	0.07 ± 0.07
stomach	1.71 ± 0.54	0.82 ± 0.24	1.34 ± 0.48	0.70 ± 0.15	0.33 ± 0.11	0.26 ± 0.04	0.29 ± 0.07	0.26 ± 0.03
intestines	1.10 ± 0.17	0.90 ± 0.14	0.49 ± 0.04	0.34 ± 0.04	1.70 ± 0.23	1.52 ± 0.16	0.88 ± 0.09	0.70 ± 0.07

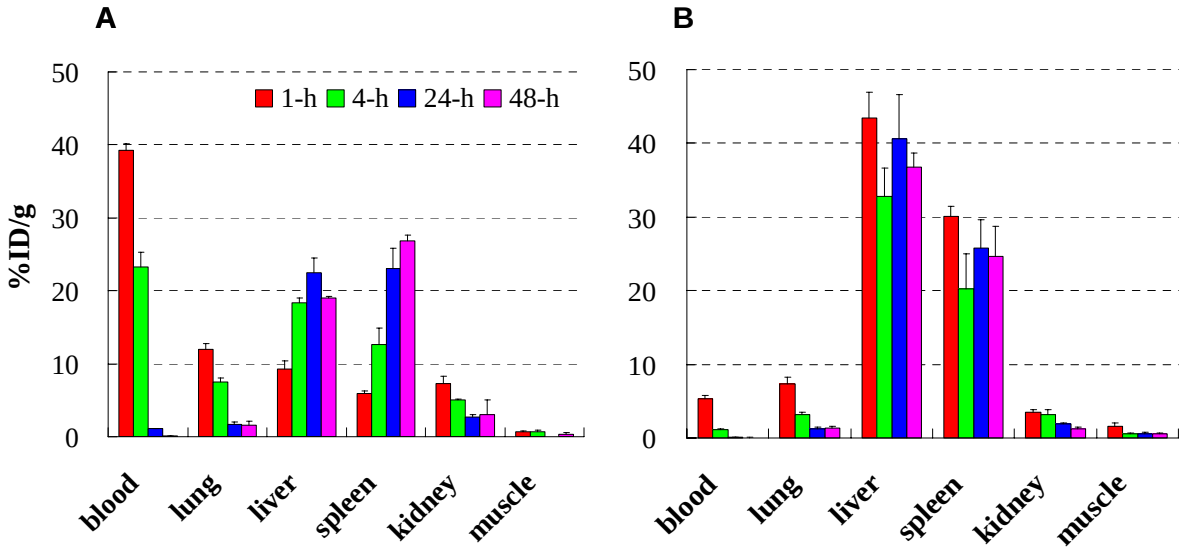

Figure 3. Biodistribution of (A) NP-1 and (B) NP-2 in normal BALB/c mice. Data are presented as measured radioactivity in blood, lung, liver, kidney and muscle (%ID/g ± s.d., n = 4).

In vivo tissue distribution of NP-1 has been evaluated in mice bearing PC-3 xenografts.

Cell culture and prostate cancer mouse model: PC3 cells were cultured in T-media (Invitrogen Corporation, Grand Island, NY) at 37° C in an atmosphere of 5% CO_2 and were passaged when reaching 75 % confluent in a P100. T-Media was supplemented with 5% Fetal Bovine Serum (Gemini Bio-Products, Woodland, CA) and 1× Penicillin/Streptomycin (Sigma, St. Louis, MO). Athymic nude mice, males (Harlan, Indianapolis, Indina) age 6-7 weeks were injected with PC3 prostate cancer cells on both rear flanks by subcutaneous injections with 1.5×10^6 cells in a 100 µL of media. The tumors were allowed to grow about 1 month until they were palpable but remained under 100 mg for the in vivo tissue distribution of NP-1.

Biodistribution: The mice bearing PC-3 tumor xenografts were separated into two groups (four mice per group) and injected intravenously via the tail vein with 100 µL of NP-1 (~ 4 µCi). Two time points (24 h and 48 h; n = 4) were used based on the above biodistribution data in normal BALB/c mice. The mice were sacrificed at 24 h and 48 h p.i. The blood, lungs, liver, spleen, kidneys, fat, muscle, heart, intestines, stomach and tumors were harvested, weighed and the radioactivity was quantified. Standards were prepared and counted along with the samples.

The biodistribution results of NP-1 in PC-3 tumor bearing mice are shown in Tables 3 and 4. The tissue distribution pattern of NP-1 in the tumor-bearing mice is similar to that in normal mice. This indicates that normal animals could be used to select ideal nano-conjugates for further evaluations. Indeed, NP-1 showed considerable uptake in tumor at 24 h (2.20 ± 0.83 %ID/g) and 48 h (1.18 ± 0.39 %ID/g) p.i., and the ratios of tumor to muscle or blood were all above ten (median values). These high contrast ratios manifested the great potential of such nanoparticles to be used as dual modality imaging agents in the detection of prostate cancer.

Table 3. The biodistribution of NP-1 in PC-3 tumor bearing mice (n = 4). Data are presented as %ID/g ± s.d. and %ID/organ ± s.d.

organ	%ID/g		%ID/organ	
	24 h	48 h	24 h	48 h
blood	0.17 ± 0.01	0.03 ± 0.02	0.33 ± 0.03	0.07 ± 0.04
lung	0.99 ± 0.27	0.94 ± 0.41	0.16 ± 0.05	0.15 ± 0.05
liver	14.89 ± 0.94	17.69 ± 1.44	19.95 ± 0.91	20.70 ± 2.19
spleen	27.99 ± 3.56	17.39 ± 2.02	2.06 ± 0.79	1.85 ± 0.22
kidney	2.13 ± 0.15	1.83 ± 0.27	0.86 ± 0.16	0.72 ± 0.07
muscle	0.21 ± 0.29	0.07 ± 0.05	0.84 ± 1.45	0.77 ± 0.57
fat	0.11 ± 0.05	0.14 ± 0.13	0.42 ± 0.20	0.53 ± 0.47
heart	0.34 ± 0.11	0.38 ± 0.04	0.04 ± 0.01	0.04 ± 0.01
stomach	0.54 ± 0.26	0.52 ± 0.14	0.25 ± 0.11	0.19 ± 0.04
intestines	0.25 ± 0.07	0.34 ± 0.11	0.67 ± 0.13	0.91 ± 0.24
tumor	2.20 ± 0.83	1.18 ± 0.39		

Table 4. Tumor to blood and tumor to muscle ratio at 24 h and 48 h p.i.

	24 h	48 h
tumor / muscle (T/M)	12.11 ± 3.87	13.30 ± 5.89
tumor / blood (T/B)	12.89 ± 3.92	31.63 ± 17.34

Key Research Accomplishments

1. A rigorous synthetic protocol has been established to prepare T10-coated nanoparticle reproducibly and in a size controllable manner.
2. Methods have been well developed for nanoparticle characterization (e.g. HPLC, DLS, SEM, TEM, and AFM).
3. In vitro stability of the prepared dextran-coated nanoparticle has been evaluated (both NP-1 and NP-2 showed excellent stability in rat serum and saline out to 72 hours).
4. The magnetic relaxivity values of the prepared dextran-coated nanoparticles have been determined.
5. Conjugation protocol of T10-coated nanoparticles (NP-1 and NP-2) with prostate cancer targeting molecules has been established.

6. In vivo tissue distribution of both NP-1 and NP-2 has been evaluated in normal mice. The nanoparticle that showed optimal biodistribution profile has been further evaluated in mice bearing PC-3 xenaografts.
7. NP-1 showed high tumor uptake and high ratios of tumor/muscle tumor/blood. In addition NP-1 exhibited a high r2/r1 ratio.

In summary, the above results clearly demonstrate the potential of NP-1 as dual modality (MRI/PET or MRI/SPECT) imaging agents for the diagnosis of prostate cancer.

Reportable Outcomes

The above results were orally presented in the DOD IMPaCT meeting in Atlanta, Georgia, September 5 – 8, 2007.
One manuscript in preparation is to be submitted next month.

Conclusions

In the second year, we have successfully prepared dextran T10-coated iron oxide nanoparticles with uniform size distribution and better controllable reproducibility compared to the 64-76 KDa dextran-coated nanoparticles reported in the first year. The radioisotope incorporation ratios for a typical PET isotope, ^{64}Cu, and a SPECT isotope, ^{177}Lu, were about 50% and 73 %, respectively, with a total preparation time of 4 hours. In addition, conjugation of nanoparticles with a prostate cancer targeting peptide, NH_2-G-R11, has been successfully carried out. In the in vitro and in vivo evaluation studies, two nanoparticles with mean sizes of 11.8 and 30.6 nm (radii) were used. The relaxivity values (r2) of the prepared nanoparticles were observed up to 43.3 $mM^{-1}s^{-1}$ with the r2/r1 ratio being 88.4, exhibiting potential application of contrast enhancement on T2- and T2*-weighted MR images. Both of the nanoparticles showed excellent in vitro stability (> 92% intact in rat serum and > 99% intact in PBS buffer out to 72 h). The biodistribution studies in normal BALB/c mice showed that the smaller nanoparticle (NP-1, radius 11.8 nm) had better tissue distribution (higher blood uptake and less accumulation in liver and spleen) than the larger one (NP-1, radius 30.6 nm). Impressively, NP-1 showed remarkable tumor uptake in a subcutaneous PC-3 xenograft mouse model with a tumor to muscle ratio of 12.11 ± 3.87 at 24 h post injection.